

# Magnetic Helicity and the Relaxation of Fossil Fields

A. E. Broderick<sup>1\*</sup> and R. Narayan<sup>1\*</sup>

<sup>1</sup> *Institute for Theory and Computation, Harvard-Smithsonian Center for Astrophysics, MS 51, 60 Garden Street, Cambridge, MA 02138, USA*

7 January 2019

## ABSTRACT

In the absence of an active dynamo, purely poloidal magnetic field configurations are unstable to large-scale dynamical perturbations and ultimately reconnect away on Alfvénic timescales. Nevertheless, there are a number of classes of stars, including Ap stars, white dwarfs, and neutron stars which are thought to not contain active dynamos and yet do exhibit significant, large scale, surface magnetic fields. Braithwaite & Spruit (2004) have shown via simulations that the external poloidal magnetic field may be stabilized in such systems by a toroidal component in the stellar interior. We present a variational principle for computing the structure of a magnetic field within a conducting sphere surrounded by an insulating vacuum. We find a simple class of axisymmetric solutions parametrized by angular and radial quantum numbers. We discuss the implications that these may have for soft-gamma repeaters and pulsar magnetic field decay.

**Key words:** stars:magnetic fields, stars:flare, stars:neutron, white dwarfs

## 1 INTRODUCTION

The importance of magnetic helicity has long been appreciated in the context of force-free plasma dynamics (Woltjer 1958, 1962). This is due primarily to the fact that it has been experimentally shown to be conserved during magnetic reconnection (Taylor 1974; Ji et al. 1995; Heidbrink & Dang 2000; Hsu & Bellan 2002). This is true even when a substantial fraction of the magnetic energy, which is not conserved, has been dissipated.

Recently, numerical magnetohydrodynamics simulations of initially random fossil fields in a conductive star have shown that magnetic helicity plays a crucial role in determining the final magnetic configuration (Braithwaite & Spruit 2004). In particular, after a period of violent reconnection, which occurs on the Alfvén crossing timescale, a stable, mostly dipolar field develops, the strength of which depends solely upon the initial helicity. In the absence of initial helicity, the final magnetic field vanishes. This result implies that the observed magnetic fields in stars without active magnetic dynamos are a one-parameter family of solutions dictated by the initial magnetic helicity alone. Relevant systems include both main-sequence stars without convection, e.g., A stars, as well as stellar remnants such as white dwarfs and neutron stars.

The simplicity of the final solution (and those found via other methods, e.g., Yoshida et al. 2006) suggests that a simple analytical model can be developed. We present a

set of magnetic field solutions as a function of the magnetic helicity obtained via a variational energy principle. These solutions are qualitatively similar to the field configurations found in Braithwaite & Spruit (2004) and naturally explain the dominance of the dipole component.

In section 2 we state the variational principle and derive the governing field equations. Section 3 solves these equations assuming axisymmetry and discusses the long term evolution of the resulting magnetic field. Explicit forms for some illustrative solutions are given in section 3.6. Section 4 contains applications to neutron star, white dwarf and Ap star magnetic field evolution, and Section 5 summarizes our conclusions.

## 2 HELICITY, MINIMUM ENERGY, AND THE FORCE-FREE CONDITION

The magnetic helicity density is defined by  $h \equiv \mathbf{A} \cdot \mathbf{B}$ , where  $\mathbf{B} \equiv \nabla \times \mathbf{A}$  is the magnetic field and  $\mathbf{A}$  is the vector potential. Generally,  $h$  is gauge dependent. Nevertheless, the volume integrated helicity can be made gauge independent by a suitable choice of integration. That is,

$$H \equiv \int_V \frac{1}{8\pi} \mathbf{A} \cdot \mathbf{B} \, d^3x, \quad (1)$$

is gauge invariant if  $\mathbf{B} \cdot d\mathbf{S} = 0$  everywhere on the boundary of  $V$ , which we denote  $\partial V$ . While during reconnection the local helicity density is not conserved, to a good approximation the total helicity is (Taylor 1974). Therefore,  $H$  is a globally important quantity in determining the final magnetic field configuration.

\* E-mail: abroderick@cfa.harvard.edu (AEB);  
rnarayan@cfa.harvard.edu (RN)

In contrast to the helicity, the magnetic energy,

$$U \equiv \int_V \frac{1}{8\pi} \mathbf{B} \cdot \mathbf{B} \, d^3x, \quad (2)$$

is not conserved during reconnection. Indeed, reconnection can convert a substantial fraction of the magnetic energy into thermal energy of the plasma. As a result, in the absence of a dynamo, the equilibrium state of the field will be associated with its minimum energy states. That is, reconnection will proceed until the maximum amount of magnetic energy is converted into heat. In the absence of other constraints the entirety of the magnetic energy will be converted. However, even under randomly chosen initial conditions, a non-zero helicity will initially be present, and subsequently must be conserved. Thus, the energy must be minimized subject to the constraint that the total helicity remain unchanged, and hence the final configuration must consist of a non-vanishing magnetic field. This situation naturally lends itself to a variational approach, which we will explore in the following subsections.

Woltjer (1958) demonstrated that in the context of uniform media a variational analysis results in the force-free equation,

$$\nabla \times \mathbf{B} = \alpha \mathbf{B}, \quad (3)$$

where  $\alpha$  is a Lagrange multiplier (Appendix A). Such a field configuration is known as a Woltjer state. The situation is more complicated if there are constraints upon the currents that can be driven in the conducting material. The simplest case, and the one of particular interest here, is when the region under consideration can be separated into regions of infinite and vanishing conductivity. Note that this corresponds to the simulations performed by Braithwaite & Spruit (2004) in which the interior of the star was taken to be infinitely conductive while the vacuum exterior was insulating.

In this situation the standard variational principle for uniform media is extended by the inclusion of Lagrange multipliers  $\alpha$  and  $\lambda(\mathbf{x})$ :

$$S = \int_V \frac{1}{8\pi} \left( \mathbf{B} \cdot \mathbf{B} - \alpha \mathbf{A} \cdot \mathbf{B} + \frac{8\pi}{c} f \lambda \cdot \mathbf{J} \right) d^3x, \quad (4)$$

where the current is related to the magnetic field in the normal way,  $\mathbf{J} \equiv c \nabla \times \mathbf{B} / 4\pi$ , and  $f(\mathbf{x})$  vanishes in regions of infinite conductivity (type-I regions) and is unity otherwise (type-II regions). Note that, unlike  $\alpha$ , which corresponds to fixing  $H$ , the  $\lambda$  are functions of position, the difference corresponding to the global versus local nature of their respective constraints.

Varying  $S$  with respect to  $\mathbf{A}$ , holding  $\delta \mathbf{A}$  fixed on some outer boundary (*not* on the boundaries between type-I and type-II regions) produces

$$\nabla \times \mathbf{B} = \alpha \mathbf{B} - \nabla \times \nabla \times f \lambda, \quad (5)$$

and varying with respect to  $\lambda$  gives

$$f \nabla \times \mathbf{B} = 0. \quad (6)$$

Within type-I ( $f = 0$ ) regions, equations (5) & (6) reduce identically to equations (3). In contrast, within type-II ( $f = 1$ ) regions, the additional terms are required to make equations (5) and (6) consistent with each other. In particular, inserting the latter into the former gives

$$\alpha \mathbf{B} = \nabla \times \nabla \times \lambda \quad (7)$$

and thus, in the interior of type-II regions,  $\nabla \times \nabla \times \lambda = \alpha \mathbf{B}$ . This implies that

$$\nabla \times \lambda = \alpha \mathbf{A} + \alpha \nabla \Lambda \quad (8)$$

for some  $\Lambda$ , the explicit form of which depends upon the gauge choices for  $\mathbf{A}$  and  $\lambda$ . A natural gauge for the former is the so-called Force-Free Gauge in which  $\mathbf{B} = \alpha \mathbf{A}$  (see Appendix A). Note that this is also a Lorentz gauge (i.e., since we are concerned with stationary solutions,  $\nabla \cdot \mathbf{A} = 0$ ).

As discussed in detail in Appendix B, the discontinuous nature of  $f$  at the boundaries between type-I and type-II regions implies the standard set of boundary conditions:

$$\begin{aligned} \hat{\mathbf{n}} \cdot (\mathbf{B}_I - \mathbf{B}_{II}) &= 0, \\ \hat{\mathbf{n}} \times (\mathbf{B}_I - \mathbf{B}_{II}) &= \frac{4\pi}{c} \mathbf{K}. \end{aligned} \quad (9)$$

Generally, for each choice of  $\alpha$  and  $\Lambda$ , a family of solutions which are local minima of magnetic energy subject to the helicity constraint may be produced. The global minimum can then be found by inspection.

In the case of a uniform medium it is possible to show that generally the magnetic energy and helicity are related by  $U = \alpha H$ . In contrast, for non-uniform media no general relation exists. This is because the force-free gauge is not generally a Lorentz gauge in the type-II regions. However, we can parametrize the departure from the uniform-medium expression in terms of the gauge transformation that relates a Lorentz gauge in the type-II regions to that determined by the continuity of  $\mathbf{A}$  at the boundaries.

In particular, let  $\varphi$  be the field potential of the magnetic field in type-II regions (i.e.,  $\mathbf{B} = \nabla \varphi$ ) and  $\Lambda_L$  be a gauge function which relates  $\mathbf{A}$  to the Lorentz gauge in type-II regions (i.e.,  $\mathbf{A} = \mathbf{A}_L + \nabla \Lambda_L$  where  $\nabla \cdot \mathbf{A}_L = 0$ ). Then, as shown in Appendix C,  $U$  and  $H$  are related by

$$U - \alpha H = \int_{\partial(I-II)} \frac{\alpha}{8\pi} (\Lambda_L \nabla \varphi - \varphi \nabla \Lambda_L) \cdot d\mathbf{S}, \quad (10)$$

which may be identified as the action.

### 3 AXISYMMETRIC SOLUTION

The discussion in the preceeding section was fairly general. However, in the context of stellar magnetic field evolution, the case of interest is the magnetic field of a spherical conducting region surrounded by an insulating vacuum. Therefore, henceforth we will restrict our attention to the case in which

$$f(\mathbf{x}) = \begin{cases} 0 & \text{if } |\mathbf{x}| \leq R, \\ 1 & \text{otherwise,} \end{cases} \quad (11)$$

where  $R$  is the stellar radius. We will explicitly construct the solution using vector spherical harmonics (Appendix D):

$$\mathbf{Y}_{lm} \equiv \hat{\mathbf{e}}_r Y_{lm}, \quad \mathbf{\Psi}_{lm} \equiv r \nabla Y_{lm}, \quad \mathbf{\Phi}_{lm} \equiv \mathbf{r} \times \nabla Y_{lm}, \quad (12)$$

and make the further simplification of assuming that the final solution is axisymmetric.

Assuming axisymmetry simplifies the computation of the force-free solutions considerably, since the magnetic field can generally be written as

$$\mathbf{B} = \nabla \times \left( A^\phi \hat{\mathbf{e}}_\phi \right) + B^\phi \hat{\mathbf{e}}_\phi. \quad (13)$$

The general procedure consists of solving for  $A^\phi$  and  $B^\phi$  for a force-free magnetic field in the stellar interior and matching this to a vacuum field in the exterior.

### 3.1 Vacuum Exterior

In the exterior, the magnetic field is defined by equations (13) and (6):

$$\nabla \times \mathbf{B} = \nabla \times \nabla \times (A^\phi \hat{\mathbf{e}}_\phi) + \nabla \times (B^\phi \hat{\mathbf{e}}_\phi) = 0. \quad (14)$$

Expanding  $A^\phi \hat{\mathbf{e}}_\phi$  and  $B^\phi \hat{\mathbf{e}}_\phi$  in terms of the vector spherical harmonics:

$$A^\phi \hat{\mathbf{e}}_\phi = \sum_l \mathcal{A}_l \Phi_l, \quad B^\phi \hat{\mathbf{e}}_\phi = \sum_l \mathcal{B}_l \Phi_l, \quad (15)$$

where in axisymmetry  $m = 0$ , and thus the azimuthal quantum number has been dropped, gives

$$\Delta_l \mathcal{A}_l = 0, \quad \mathcal{B}_l = 0, \quad (16)$$

which has the general solution

$$\mathcal{A}_l = \frac{a_l}{r^{l+1}} + b_l r^l. \quad (17)$$

Regularity at infinity requires  $b_l = 0$ , and thus

$$\mathbf{B} = \sum_l \left[ -l(l+1) \frac{a_l}{r^{l+2}} \mathbf{Y}_l + l \frac{a_l}{r^{l+2}} \Psi_l \right]. \quad (18)$$

### 3.2 Stellar Interior

In the stellar interior it is possible to make use of the force-free gauge ( $\mathbf{B} = \alpha \mathbf{A}$ ), and rewrite  $\mathbf{B}$  in terms of  $B^\phi$  alone:

$$\mathbf{B} = \alpha^{-1} \nabla \times (B^\phi \hat{\mathbf{e}}_\phi) + B^\phi \hat{\mathbf{e}}_\phi. \quad (19)$$

$B^\phi \hat{\mathbf{e}}_\phi$  may again be expanded in the vector spherical harmonics as before, with the result that the force-free equation is

$$\nabla \times \nabla \times \sum_l \mathcal{B}_l \Phi_l = \alpha \sum_l \mathcal{B}_l \Phi_l, \quad (20)$$

which upon making use of the properties of the vector spherical harmonics gives

$$\Delta_l \mathcal{B}_l + \alpha^2 \mathcal{B}_l = 0. \quad (21)$$

The general solution of equation (21) can be written in terms of spherical Bessel functions:

$$\mathcal{B}_l = \alpha [c_l n_l(\alpha r) + d_l j_l(\alpha r)], \quad (22)$$

where  $j_l$  and  $n_l$  are the spherical Bessel functions of the first and second kind, respectively. Regularity at the centre combined with the orthogonality of the  $n_l$  imply that the  $c_l$  must vanish. Therefore, the general solution for the axisymmetric force-free magnetic field is

$$\mathbf{B} = \sum_l \left\{ - \left[ \frac{l(l+1)}{r} d_l j_l(\alpha r) \right] \mathbf{Y}_l - \left[ \frac{1}{r} \partial_r r d_l j_l(\alpha r) \right] \Psi_l + \alpha d_l j_l(\alpha r) \Phi_l \right\}. \quad (23)$$

This must now be matched across the surface,  $|\mathbf{x}| = R$ , using the standard boundary conditions (equation 9), which relates the  $a_l$  and  $d_l$ :

$$d_l = \frac{a_l}{R^{l+1} j_l(\alpha R)}. \quad (24)$$

### 3.3 Multipole Composition

The set of field solutions in the previous subsections all satisfy the equations obtained from varying  $S$  with respect to  $\mathbf{A}$ . However, we have yet to determine the global minimum energy. That is, we have replaced the degrees of freedom associated with the functional form of  $\mathbf{B}$  with an infinite, but countable, set of degrees of freedom associated with the coefficients  $a_l$ . Furthermore, we have yet to choose an  $\alpha$ . This can be addressed by considering  $S(a_l; \alpha)$  explicitly, i.e., minimizing the energy with respect to the  $a_l$  and  $\alpha$ , subject to the constraint of fixed  $H$ .

Equation (10) provides a direct way in which to construct  $S(a_l; \alpha)$  in terms of  $\varphi$  and  $\Lambda_L$ , and thus we will determine functional forms for these now. By inspection of equation (18),

$$\varphi = \sum_l \frac{a_l l}{r^{l+1}} Y_{l0}. \quad (25)$$

Determining  $\Lambda_L$  is more difficult. Letting  $\mathbf{A} = A^\phi \hat{\mathbf{e}}_\phi$  is sufficient to produce the required vacuum field solution, and also satisfies the Lorentz gauge. However,  $\mathbf{A}$  must also be continuous across the stellar surface. Thus,  $\Lambda_L$  is defined by

$$\nabla \Lambda_L|_{r=R} = \sum_l \frac{a_l}{\alpha} \left\{ - \left[ \frac{l(l+1)}{R} j_l(\alpha R) \right] \mathbf{Y}_l + \left[ \frac{l}{R} j_l(\alpha R) - \alpha j_{l-1}(\alpha R) \right] \Psi_l \right\}, \quad (26)$$

where  $\partial_z z j_l(z) = z j_{l-1}(z) - l j_l(z)$  was used (Abramowitz & Stegun 1972). However, setting  $\Lambda_L = \sum_l \lambda_{Ll}(r) Y_{l0}(\theta, \phi)$  gives

$$\nabla \Lambda_L = \sum_l \left[ \partial_r \lambda_{Ll} \mathbf{Y}_l + \frac{\lambda_{Ll}}{r} \Psi_l \right], \quad (27)$$

which, together with the orthogonality of the vector spherical harmonics, implies

$$\lambda_{Ll} = \frac{a_l}{\alpha} \left[ \left( \frac{r}{R} \right)^{-(l+1)} l j_l(\alpha R) - \alpha R j_{l-1}(\alpha R) \right]. \quad (28)$$

Therefore, after integrating over the stellar surface,

$$S(a_l; \alpha) = \frac{\alpha}{8\pi} \sum_l a_l^2 \frac{l(l+1)}{R^{l-1}} \frac{j_{l-1}(\alpha R)}{j_l(\alpha R)}. \quad (29)$$

As expected, after simplification, variations of this with respect to  $\alpha$  gives  $H(a_l; \alpha)$  (cf. with equation 32). Variations of  $S(a_l; \alpha)$  with respect to  $a_l$  gives a new condition,

$$\alpha a_l \frac{j_{l-1}(\alpha R)}{j_l(\alpha R)} = 0, \quad (30)$$

which implies that either  $a_l = 0$  or  $j_{l-1}(\alpha R) = 0$  for all  $l$ . Since the zeros of the spherical Bessel functions are non-degenerate, at most a single multipole component can be non-vanishing. Thus a minimum energy configuration consists of a simple multipole  $l$  with  $\alpha$  selected such that  $j_{l-1}(\alpha R) = 0$ . It is worth noting that this corresponds to the poloidal component of the field being continuous at the stellar surface. That is, perhaps unsurprisingly, the minimum energy is when there is no kink in the poloidal component of the magnetic field at the surface.

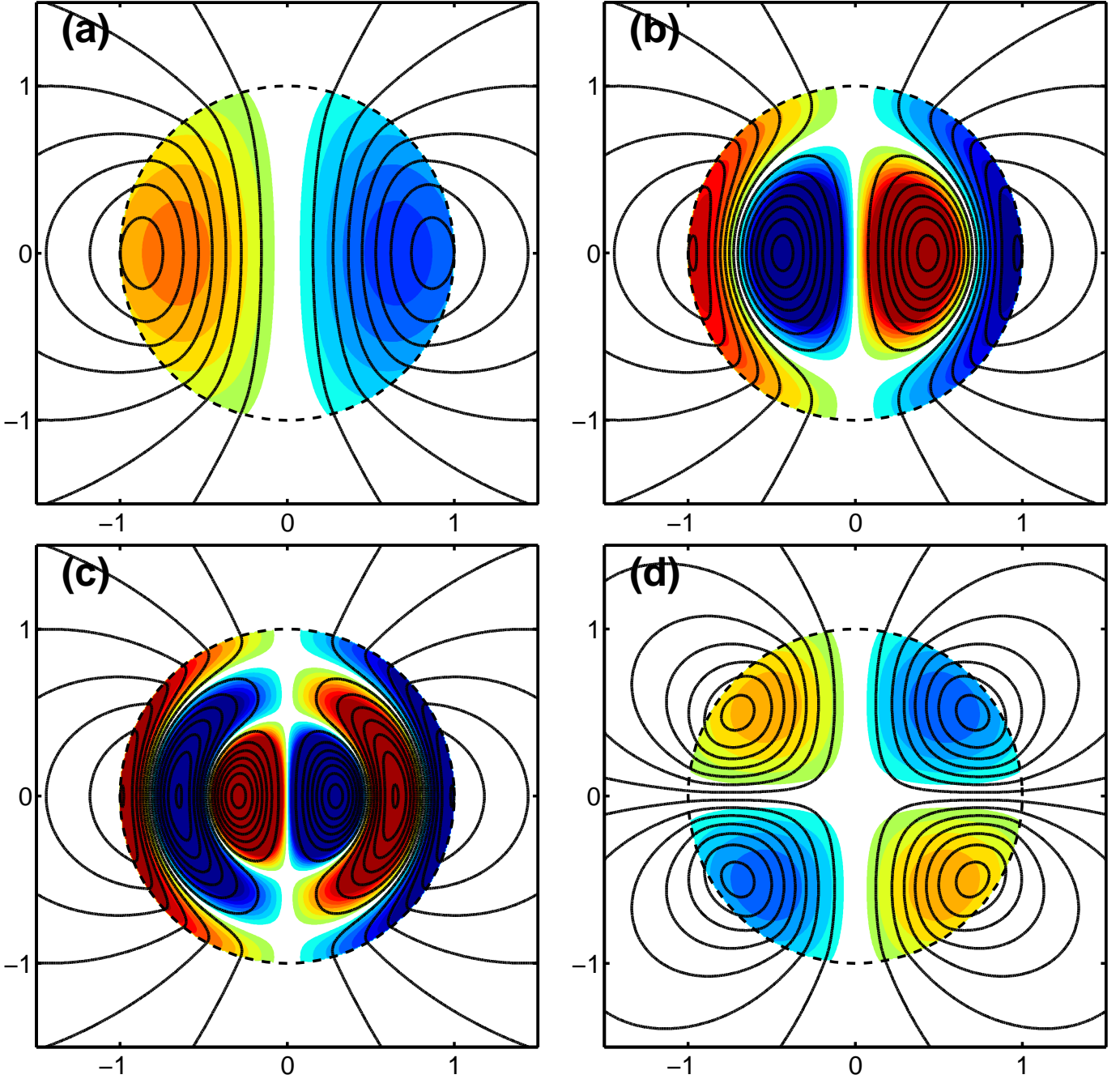


**Figure 1.** Azimuthal slices of illustrative magnetic field geometries for (a) the global minimum energy configuration, (b) & (c) the first and second local equilibrium dipole configuration and (d) the lowest energy quadrupole configuration. The poloidal and toroidal field structure is shown by the field lines and filled-color contours, respectively. In all plots the field line density is proportional to the poloidal flux and is normalized such that the average surface fields are equal. Similarly, the toroidal color scheme is uniform among all of the plots.

### 3.4 Energy and Helicity

For the values of  $a_l$  and  $\alpha$  found in the previous subsection,  $S$  identically vanishes. As a consequence, at the global energy minimum the magnetic helicity and energy are related by  $U = \alpha H$ , as found previously for Woltjer states in uniform media. After integrating equation (C1) for the magnetic energy, we find that  $U = \alpha H = l(l+1)\alpha^2 a_l^2 / 8\pi R^{l-2}$ , and thus given a fixed  $H$ , this defines the value of  $a_l$ .

The global energy minimum for a given magnetic helicity is now reduced to determining the minimum permissible  $\alpha$ , i.e., the smallest root of  $j_l(z)$  for  $l > 0$ . By inspection it is clear that this is for  $l = 1$ , and thus the lowest energy magnetic field corresponds to a dipolar configuration with  $\alpha = \pi/R$ , shown in Figure 1a. Nevertheless, there are a number of higher energy, local minima corresponding to both higher multipoles and/or more complex radial struc-

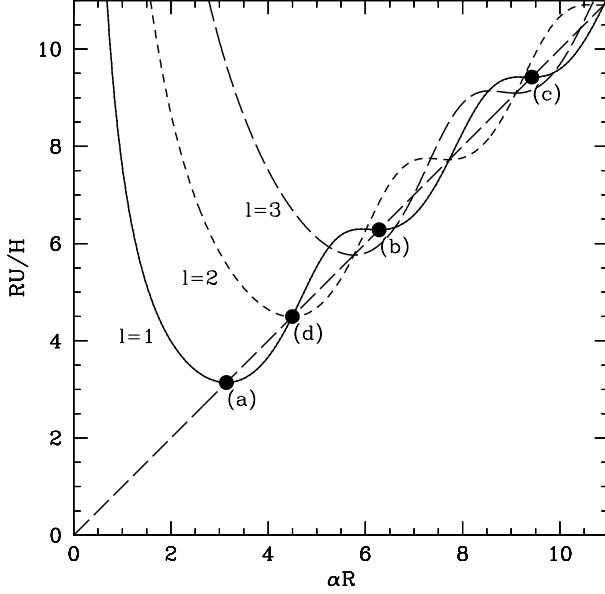


**Figure 2.** The energy per unit helicity as a function of the force-free constant,  $\alpha$  (both appropriately scaled by the stellar radius) for the first three multipoles. The dipole configuration with  $\alpha R = \pi$ , labelled (a), corresponds to the global minimum energy for a given helicity; the associated field geometry is shown in Figure 1a. There is a spectrum of higher energy local equilibria for each multipole, e.g., (b) and (c) for the dipole, corresponding to Figures 1b and 1c. The point (d) is the minimum energy quadrupole, corresponding to Figure 1d. For reference, the  $U = \alpha H$  line is shown, which also corresponds to the uniform-medium case.

tures. These are apparent in panels b–d of Figure 1, and discussed in more detail in the following section.

### 3.5 Non-Equilibrium Configurations

While we have found a globally optimized magnetic field geometry for a given magnetic helicity, thus far we have presumed that the star will naturally seek this minimum energy state via large scale motions and reconnection events. However, there is no guarantee that the star will not become trapped in higher energy, local equilibria, in which the necessary large scale rearrangements are inhibited. For this reason we consider a simple evolution, comprised of a single multipole and varying  $\alpha$ , which may occur, for instance, in some forms of current decay.

For values of  $\alpha$  which are not zeros of  $j_l(\alpha R)$  the action does not vanish. Nonetheless, it is straight forward to compute  $U$  and use  $S(\alpha R)$  to relate this to  $H(\alpha)$ :

$$U = \frac{l(l+1)}{8\pi R^{l-2}} \alpha^2 a_l^2 \left[ 1 - \frac{2l}{\alpha R} \frac{j_{l-1}(\alpha R)}{j_l(\alpha R)} + \frac{j_{l-1}^2(\alpha R)}{j_l^2(\alpha R)} \right], \quad (31)$$

$$H = \frac{U - S}{\alpha} = \frac{l(l+1)}{8\pi R^{l-2}} \alpha a_l^2 \left[ 1 - \frac{2l+1}{\alpha R} \frac{j_{l-1}(\alpha R)}{j_l(\alpha R)} + \frac{j_{l-1}^2(\alpha R)}{j_l^2(\alpha R)} \right]. \quad (32)$$

Since equilibria minimize the energy per unit helicity, we

show the quantity  $RU/H$  as a function of  $R\alpha$  for a number of multipoles in Figure 2. For each multipole there is a global minimum, with  $U/H$  being smallest for the dipole. However, also of interest is the fact that there are a number of additional local minima corresponding to higher energy states. The explicit geometry for some of these are shown in Figure 1, and their implications are discussed in Sections 3.7 and 4.

### 3.6 Explicit Expressions for the Magnetic Field

In this subsection we provide for convenience explicit expressions for the magnetic field geometries that are presented in Figures 1a, 1b and 1d. These include the global minimum energy, the first dipole local minimum and the lowest energy quadrupole geometries.

The global minimum energy solution (Figure 1a) is explicitly

$$\begin{aligned} \mathbf{B}_{r < R} = \pi B_0 \left\{ \frac{2R}{r} j_1 \left( \frac{\pi r}{R} \right) \cos \theta \hat{\mathbf{e}}_r \right. \\ \left. + \left[ \frac{R}{r} j_1 \left( \frac{\pi r}{R} \right) - \pi j_0 \left( \frac{\pi r}{R} \right) \right] \sin \theta \hat{\mathbf{e}}_\theta \right. \\ \left. + \pi j_1 \left( \frac{\pi r}{R} \right) \sin \theta \hat{\mathbf{e}}_\phi \right\}, \end{aligned} \quad (33)$$

$$\mathbf{B}_{r \geq R} = B_0 R^3 \left[ \frac{2}{r^3} \cos \theta \hat{\mathbf{e}}_r + \frac{1}{r^3} \sin \theta \hat{\mathbf{e}}_\theta \right],$$

where the explicit forms of  $\mathbf{Y}_1$ ,  $\mathbf{\Psi}_1$  and  $\mathbf{\Phi}_1$  given in Table D1 were used, the expressions for  $j_1$  and  $j_0$  may be found in Table D2, and the  $a_1$  and some fixed constants were subsumed into  $B_0$ .

The first local minimum for the dipole (Figure 1b) is given by

$$\begin{aligned} \mathbf{B}_{r < R} = 2\pi B_0 \left\{ \frac{2R}{r} j_1 \left( \frac{2\pi r}{R} \right) \cos \theta \hat{\mathbf{e}}_r \right. \\ \left. + \left[ \frac{R}{r} j_1 \left( \frac{2\pi r}{R} \right) - 2\pi j_0 \left( \frac{2\pi r}{R} \right) \right] \sin \theta \hat{\mathbf{e}}_\theta \right. \\ \left. + 2\pi j_1 \left( \frac{2\pi r}{R} \right) \sin \theta \hat{\mathbf{e}}_\phi \right\}, \end{aligned} \quad (34)$$

$$\mathbf{B}_{r \geq R} = B_0 R^3 \left[ \frac{2}{r^3} \cos \theta \hat{\mathbf{e}}_r + \frac{1}{r^3} \sin \theta \hat{\mathbf{e}}_\theta \right].$$

The lowest energy quadrupolar configuration (Figure 1d) is given by

$$\begin{aligned} \mathbf{B}_{r < R} = \frac{B_0}{j_2(z_1)} \left\{ \frac{R}{r} j_2 \left( \frac{z_1 r}{R} \right) (3 \cos^2 \theta - 1) \hat{\mathbf{e}}_r \right. \\ \left. + \left[ \frac{2R}{r} j_2 \left( \frac{z_1 r}{R} \right) - z_1 j_1 \left( \frac{z_1 r}{R} \right) \right] \cos \theta \sin \theta \hat{\mathbf{e}}_\theta \right. \\ \left. + z_1 j_2 \left( \frac{z_1 r}{R} \right) \cos \theta \sin \theta \hat{\mathbf{e}}_\phi \right\}, \end{aligned}$$

$$\mathbf{B}_{r \geq R} = B_0 R^4 \left[ \frac{1}{r^4} (3 \cos^2 \theta - 1) \hat{\mathbf{e}}_r + \frac{2}{r^4} \cos \theta \sin \theta \hat{\mathbf{e}}_\theta \right], \quad (35)$$

where  $z_1 \simeq 4.4934$  is the first root of  $j_1(z)$ .

### 3.7 Long Term Field Evolution

In the presence of a non-zero resistivity, the magnetic field will necessarily decay. Since, in practice, the resistive decay

timescales are typically much longer than the Alfvén crossing time, we may approximate the state of the magnetic field as a series of the non-equilibrium configurations discussed in the previous section, for which the general solution is given by equations (23) and (18). Furthermore, we will assume that the field began in a local minimum energy configuration, where the large-scale structure prevents further fast reconnection.

As the field evolves due to resistive decay, the energy per unit helicity,  $U/H$ , will change as well. As a consequence, the value of  $\alpha$  will evolve. This will generally result in the evolution of the magnetic field structure, provided the resistivity is not scale-invariant, i.e., small scale currents damp more rapidly than large scale currents. To see this consider Ohmic decay with a constant resistivity,  $\rho$ . In this case, the local field strength evolves according to

$$\dot{\mathbf{B}} = -\nabla \times \mathbf{E} = -\rho \nabla \times \mathbf{J} = -\frac{\rho}{4\pi} \nabla \times \nabla \times \mathbf{B} = -\frac{\alpha^2 \rho}{4\pi} \mathbf{B}. \quad (36)$$

Upon inserting equation (23) into this, we find

$$\dot{a}_l = -\frac{\alpha^2 \rho}{4\pi} a_l \quad \text{and} \quad \dot{\alpha} = 0, \quad (37)$$

i.e., the magnetic field strength (proportional to  $a_l$ ) decreases but the structure (described by  $\alpha$ ) remains unchanged.

However, if the poloidal currents decay more rapidly than the toroidal currents, e.g., due to enhanced dissipation of the surface currents or because dissipation is non-linear,  $\alpha$  will be time dependent. This is clear from equation (23), in which  $B^\phi/B^r \propto \alpha$ . Thus if poloidal currents (and hence toroidal magnetic fields) decay more rapidly than toroidal currents (and hence poloidal magnetic fields),  $\dot{\alpha} < 0$  and the magnetic field configuration will move to the left in Figure 2. When the system evolves out of a local equilibrium state a substantial amount of magnetic energy is necessarily liberated. The natural timescale over which this energy is released is the Alfvén crossing time, though we do not address the details of the instability here.

Finally, note that in the presence of a conducting magnetosphere with an infinitely conductive surface the system would appear as a uniform medium. This is despite the fact that the magnetosphere has a much lower density than the stellar interior, and thus is always described by force-free dynamics. This disparity results in very different dynamical times for the two regions. Nevertheless, since currents can freely flow between the stellar interior and the magnetosphere, the equilibrium configuration will be described by that for a uniform medium, which has no stable equilibrium magnetic field configuration for any value of magnetic helicity. That is, in this case  $\alpha = U/H$  can take any value, including zero. Thus such a field is unconditional unstable. If and when this occurs in the context of a stellar field depends upon the conductivity of the surface and exterior.

#### 4 DISCUSSION AND APPLICATIONS TO NON-CONVECTIVE STARS

A number of qualitative features of numerical simulations can be naturally explained in terms of the simple calculation presented in the preceding sections. Most significantly,

these include the dominance of the dipole field, and the presence of a substantial toroidal component within the star.

Despite the dominance of the dipole component, within the context of a magnetic relaxation model the presence of higher order multipoles is not unexpected. After the cessation of a dynamo, the resulting magnetic field will be violently unstable, decaying rapidly towards a local minimum energy configuration. However, as described in section 3.7, this will only proceed as long as this rearrangement is driven by small scale reconnection. Large scale rearrangements (such as converting low-order multipoles into dipoles) will occur over the much longer resistive timescale. As a direct consequence, we generally expect the resulting surface field to be dominated by a dipole component with significant quadrupolar and octupolar components. This is consistent with the outcome of numerical simulations (Braithwaite & Spruit 2004).

Late time evolution will be driven by small-scale current decay, presumably near the stellar surface. This will drive the system leftward of the global minimum in Figure 2, necessarily ultimately resulting in a violently unstable configuration. This also has been observed at late times in numerical simulations (Braithwaite & Spruit 2004).

A novel feature of our result is the existence of higher-energy quasi-equilibrium states, described in 3.5. At late times, small-scale current decay will drive the system to evolve towards smaller  $\alpha$ , necessarily resulting in periods of violent instability. These result in large scale reorganizations of the internal and external stellar magnetic fields over Alfvénic timescales. As a consequence, these events could power active periods in which a substantial fraction of the stellar magnetic energy is released. The manner in which this variability will be exhibited depends upon the physical parameters of the star under consideration. The timescale ranges from a second, for neutron stars, to a year for Ap stars (see below).

Since the quasi-equilibria of the dipole state are located at  $\alpha = n\pi$ , the magnetic energy release in these events should be roughly quantized (though the system may jump over many local equilibria in a single event), releasing an energy of roughly  $k\pi H/R$  for some integer  $k$ . The observed energy release will depend strongly upon the emission mechanism and will likely not appear strictly quantized. Nevertheless, this model implies a lower limit upon the energy that can be released during an outburst, simply given by the energy of the global minimum energy configuration.

#### 4.1 Neutron Stars

During their birth, neutron stars are expected to develop extremely strong magnetic fields, as high as  $10^{15-16}$  G. However, shortly afterward, and prior to the development of an insulating crust, the nascent neutron star magnetic field must evolve in the absence of an active dynamo for on the order of  $10^4$  Alfvén crossing times (roughly 100 s). During this time magnetic relaxation will play a central role in determining the strength and structure of the magnetic field that is subsequently frozen into the star.

Generally, we expect a dominantly dipole field structure, with non-negligible quadrupole and octupole components. Note that because the magnetic helicity is a *scalar* quantity, this provides a natural way in which to produce

non-aligned magnetic fields. In this case, for a highly tangled initial field (with considerable power on small-scales), the orientation of the birth fields of neutron stars would be uniformly distributed relative to the spin axis. This provides a natural way in which to produce the off-axis fields required for pulsars.

Outbursts associated with the evolution of the high-energy quasi-equilibrium states provide a natural mechanism for powering bursts associated with soft-gamma repeaters (SGRs). With typical energies ranging from  $10^{36-46}$  erg, SGR bursts would require interior magnetic fields on the order of  $10^{9-14}$  G, which are considerably less than the equipartition values that are possible as a result of magnetar formation (Thompson & Duncan 1993; Spruit 2002). For magnetars, the Alfvén crossing time is on the order of a second, corresponding to maximum luminosities on the order of  $10^{46}$  erg/s. If this energy is thermalized in the neutron star crust over the Alfvén timescale, it would result in surface temperatures on the order of roughly an MeV, appearing quite similar to an SGR flare. However, the precise details of the emission will depend upon the details of the emission mechanism (see, e.g., Thompson et al. 2002; Lyutikov 2006).

In this picture magnetars are born with magnetic fields in configurations that are local equilibria at strengths orders of magnitude larger than the global minimum. If we assume that the minimum energy of observed SGR bursts is indicative of the energy scale of the power source, this implies that the field strength in this minimum energy state is roughly  $10^9$  G. Hence, the SGR bursts would be the result of the decay of the internal magnetic field, resulting finally in a stable field strength commensurate with millisecond pulsars. Note that this is a different mechanism than that described in Braithwaite & Spruit (2006).

If neutron stars with strong magnetic fields  $\gtrsim 10^9$  G are indeed supported by helicity conservation, this may provide an intriguing explanation for magnetic field decay in accreting systems. In the presence of a highly conducting magnetosphere, the nature of the magnetic field structure will depend upon the conductivity of the neutron star crust. If it is insulating, the internal currents supporting the toroidal field will be unable to escape the surface, producing an identical interior configuration to the situation analysed in this paper. However, if the crust is perfectly conducting, currents will pass freely between the interior and exterior of the star, producing a force-free field everywhere. In this case there are *no minima*, and the magnetic field energy may vanish for a fixed helicity. Therefore, in this context magnetic field decay may be a function primarily of crustal conductivity, and thus surface temperature. This might provide a natural way in which to shorten the field decay timescales for accreting neutron stars, as is implied by the low surface fields of millisecond pulsars.

## 4.2 White Dwarfs

A subpopulation of white dwarfs exhibit strong magnetic fields ( $B \simeq 10^{6-9}$  G). They are typically more massive than non-magnetic white dwarfs, with  $M \sim 0.9M_{\odot}$  (Wickramasinghe & Ferrario 2005). Observations of their surface magnetic fields suggest that they are dominantly dipolar, with sub-dominant, though non-negligible higher harmonics, well

fit by an offset dipole model. For this reason, many of the observational consequences of the magnetic relaxation model for neutron stars are expected in this case as well. Specifically, white dwarfs should exhibit an offset dipole field with periods of substantial activity.

However, in comparison to the neutron star, the Alfvén crossing timescale is considerably longer, typically on the scale of hours to months. The typical energy released during outbursts of highly magnetized white dwarfs is on the order of  $10^{44}$  erg and comparable to those from SGRs. If this energy were thermalized over the Alfvénic timescales, it would result in surface temperatures on the order of 100 eV, well into the hard-UV/soft-X-ray, and thus unlikely to be observed directly. Nevertheless, the impulsive release of this much energy at ionizing wavelengths will likely unbind the white dwarf photosphere, shocking the surrounding interstellar material producing possibly observable results.

## 4.3 Ap stars

The surface fields of Ap stars share many of the observational features of magnetized white dwarfs (see, e.g., Landstreet & Mathys 2000), leading some to conclude that there is an evolutionary relationship between the two (Tout et al. 2004). The field strengths are considerably lower in Ap stars, roughly  $10^4$  G, and are well fit by an offset dipolar field.

Again we expect periods of activity as high-energy, quasi-equilibrium magnetic field configurations evolve towards the lowest energy equilibrium. In this case the typical Alfvén crossing time is on the order of a year, producing luminosities on the order of  $10^{34}$  erg/s  $\simeq 10L_{\odot}$ , over this timescale. Thus, if Ap stars are trapped in high-energy, quasi-equilibrium states, we expect periods of significant enhancement of the stellar luminosity. However, the frequency with which these occur is not presently clear, and based upon that observed in their neutron star analogs, SGRs, may be quite small.

## 5 CONCLUSIONS

A simple variational principle is capable of reproducing many features of recent numerical simulations of the evolution of initially random stellar magnetic fields. We have explicitly ignored the effect of a magnetosphere, and the dynamics associated with the relaxation process. Nevertheless, we are able to explain many of the observed features of stars that do not have active dynamos.

In particular, natural consequences of the magnetic relaxation model described here include stable dominantly dipolar field configurations with non-negligible higher multipoles, and non-aligned magnetic fields (required for pulsars). In addition, the model may explain SGR bursts as periods of violent relaxation as neutron star magnetic fields transition between quasi-equilibrium states. Given the generality of this result, we suggest that similar behavior may be present also in white dwarfs and Ap stars, though at substantially different luminosities, energies and timescales.

**ACKNOWLEDGEMENTS**

This work was supported in part by NASA grant NNG04GL38G. A.E.B. gratefully acknowledges the support of an ITC Fellowship from Harvard College Observatory. A.E.B would also like to thank Jon McKinney and Niayesh Afshordi for a number of useful discussions.

**APPENDIX A: FORCE-FREE FIELDS IN UNIFORM MEDIA**

When the medium is uniformly infinitely conductive (i.e., the currents required by the resulting magnetic field satisfy any physical restrictions) the quantity to be minimized is

$$S = \int_V \frac{1}{8\pi} (\mathbf{B} \cdot \mathbf{B} - \alpha \mathbf{A} \cdot \mathbf{B}) d^3x, \quad (\text{A1})$$

where the constraint upon the total helicity is included via the Lagrange multiplier  $\alpha$ . As originally discussed in Woltjer (1958) (and thus frequently referred to as the Woltjer state) variations with respect to  $\mathbf{A}$  produce the familiar force-free equation  $\nabla \times \mathbf{B} = \alpha \mathbf{B}$  for the magnetic field. That this produces a force-free field is not unexpected; non-force-free perturbations to a force-free solution necessarily require work to be done upon, and thus energy added to, the magnetic field. For the purpose of comparison with what follows we will derive this equation below.

First note that

$$\begin{aligned} \delta(\mathbf{B} \cdot \mathbf{B}) &= 2\delta\mathbf{A} \cdot (\nabla \times \mathbf{B}) - 2\nabla \cdot (\mathbf{B} \times \delta\mathbf{A}), \\ \delta(\mathbf{A} \cdot \mathbf{B}) &= 2\delta\mathbf{A} \cdot (\nabla \times \mathbf{A}) - \nabla \cdot (\mathbf{A} \times \delta\mathbf{A}). \end{aligned} \quad (\text{A2})$$

Therefore,

$$\begin{aligned} 8\pi\delta S &= \int_V \delta\mathbf{A} \cdot (\nabla \times \mathbf{B} - \alpha \nabla \times \mathbf{A}) d^3x \\ &\quad - \int_{\partial V} \left( \mathbf{B} \times \delta\mathbf{A} - \frac{\alpha}{2} \mathbf{A} \times \delta\mathbf{A} \right) \cdot d\mathbf{S} \\ &= \int_V \delta\mathbf{A} \cdot (\nabla \times \mathbf{B} - \alpha \mathbf{B}) d^3x \\ &\quad - \int_{\partial V} \delta\mathbf{A} \cdot \left[ \hat{\mathbf{n}} \times \left( \mathbf{B} - \frac{\alpha}{2} \mathbf{A} \right) \right] d^2x, \end{aligned} \quad (\text{A3})$$

where  $\hat{\mathbf{n}}$  is the normal to the surface defined by  $\partial V$  and  $d^2x$  is defined by  $d\mathbf{S} \equiv \hat{\mathbf{n}} d^2x$ . Note that the surface integral is generally gauge dependent. This can be cured if  $\delta\mathbf{A}$  is constrained to vanish at  $\partial V$ . Since in what follows we will set  $\partial V$  to infinity and the energy in the field will necessarily be finite, a gauge will necessarily exist in which  $\mathbf{A}$  vanishes on  $\partial V$ , and thus this constraint upon  $\partial V$  is justified. Therefore, the desired magnetic field must satisfy

$$\nabla \times \mathbf{B} = \alpha \mathbf{B}. \quad (\text{A4})$$

Equation (A4) implies that

$$\nabla \times (\mathbf{B} - \alpha \mathbf{A}) = 0 \quad \rightarrow \quad \alpha \mathbf{A} = \mathbf{B} + \alpha \nabla \Lambda, \quad (\text{A5})$$

and thus a natural gauge choice for non-zero  $\alpha$  is the “force-free” gauge defined by  $\Lambda = 0$ . Note that this is also a Lorentz gauge since  $\nabla \cdot \mathbf{B} = 0$ .

Within the force-free gauge it is straightforward to show that the helicity and minimum possible magnetic energy are proportional. That is,

$$H = \int_V \frac{1}{8\pi} \mathbf{A} \cdot \mathbf{B} d^3x = \int_V \frac{1}{8\pi} \alpha^{-1} \mathbf{B} \cdot \mathbf{B} d^3x = \alpha^{-1} U, \quad (\text{A6})$$

and thus small  $\alpha$  correspond to small  $U$  for the same  $H$ .

**APPENDIX B: BOUNDARY CONDITIONS**

On the boundaries between type-I and type-II regions, the fields must satisfy the usual boundary conditions:

$$\hat{\mathbf{n}} \cdot (\mathbf{B}_I - \mathbf{B}_{II}) = 0 \quad \text{and} \quad \hat{\mathbf{n}} \times (\mathbf{B}_I - \mathbf{B}_{II}) = \frac{4\pi}{c} \mathbf{K}, \quad (\text{B1})$$

where  $\hat{\mathbf{n}}$  is the surface normal (directed from I to II) and  $\mathbf{K}$  is the induced surface current density. The proper surface current can be found by explicitly constructing solutions and minimizing the magnetic energy. Note that this ignores any energy associated with the surface currents themselves.

However, this should also emerge naturally from the equations (5) and (6). The first is obtained from  $\nabla \cdot \mathbf{B} = 0$ , which is true by definition and may be verified by taking the divergence of equation (5). The second is obtained via integrating equation (5) around an infinitesimal loop crossing the surface. Define a local Cartesian coordinate system at the position of interest at the I-II boundary in which  $\hat{\mathbf{z}} \parallel \hat{\mathbf{n}}$  at the boundary, at which  $z = 0$ . Then, upon integrating around a rectangular loop in the  $x$ - $z$  plane of length  $\ell$  in the  $\hat{\mathbf{x}}$ -direction and vanishing length in the  $\hat{\mathbf{z}}$ -direction, we find

$$\begin{aligned} (\mathbf{B}_I - \mathbf{B}_{II}) \cdot \ell \hat{\mathbf{x}} &= \int_C \mathbf{B} \cdot d\boldsymbol{\ell} = \int_A (\nabla \times \mathbf{B}) \cdot d\mathbf{S} \\ &= \int_A (\alpha \mathbf{B} - \nabla \times \nabla \times f \boldsymbol{\Lambda}) \cdot d\mathbf{S} \\ &= \int_C (\alpha \mathbf{A} + \boldsymbol{\Lambda} \times \nabla f - f \nabla \times \boldsymbol{\Lambda}) \cdot d\boldsymbol{\ell} \\ &= \int_C [(1-f)\alpha \mathbf{A} - f\alpha \nabla \Lambda + \boldsymbol{\Lambda} \times \nabla f] \cdot d\boldsymbol{\ell}. \end{aligned} \quad (\text{B2})$$

The third term in the integrand can be integrating after noting  $\nabla f = \hat{\mathbf{z}} \delta(z)$  by definition, and thus

$$\int_C \delta(z) \boldsymbol{\Lambda} \times \hat{\mathbf{z}} \cdot d\boldsymbol{\ell} = (\boldsymbol{\Lambda} \times \hat{\mathbf{z}}) \cdot \hat{\mathbf{z}} = 0. \quad (\text{B3})$$

Despite the explicit presence of the vector potential, the first two terms in the integrand are indeed gauge independent. Explicitly, note that since under the gauge transformation  $\mathbf{A} \rightarrow \mathbf{A} + \nabla \Lambda'$  also implies that  $\Lambda \rightarrow \Lambda - \Lambda'$ , and hence

$$(1-f)\alpha \mathbf{A} - f\alpha \nabla \Lambda \rightarrow (1-f)\alpha \mathbf{A} - f\alpha \nabla \Lambda + \nabla \Lambda'. \quad (\text{B4})$$

Finally, noting that  $\int_C \nabla \Lambda' \cdot d\boldsymbol{\ell} = 0$  completes the proof.

Therefore,

$$(\mathbf{B}_I - \mathbf{B}_{II}) \cdot \ell \hat{\mathbf{x}} = \alpha \mathbf{A}_I \cdot \ell \hat{\mathbf{x}} + \alpha \ell \hat{\mathbf{x}} \cdot \nabla \Lambda \quad (\text{B5})$$

With an analogous expression for a loop in the  $y$ - $z$  plane, the surface current is given by

$$\frac{4\pi}{c} \mathbf{K} = \alpha \hat{\mathbf{n}} \times (\mathbf{A}_I + \nabla \Lambda). \quad (\text{B6})$$

If we choose the force-free gauge within regions of type-I, continuity of the vector potential gives

$$\frac{4\pi}{c} \mathbf{K} = \hat{\mathbf{n}} \times (\mathbf{B}_I + \alpha \nabla \Lambda), \quad (\text{B7})$$

or,

$$\hat{\mathbf{n}} \times (\mathbf{B}_{II} - \alpha \nabla \Lambda) = 0, \quad (\text{B8})$$

on the boundary. That is, as expected  $\mathbf{B}_{II}$  is a potential field, though otherwise the surface currents are unconstrained.



### APPENDIX C: THE ACTION IN NON-UNIFORM MEDIA

In non-uniform medium, it is possible to explicitly reduce the computation of the action to integrals over the boundaries between conducting (type-I) and insulating (type-II) regions. To do this, first note that the magnetic energy is given by

$$\begin{aligned} U &= \int_I \frac{1}{8\pi} \mathbf{B} \cdot \mathbf{B} \, d^3x + \int_{II} \frac{1}{8\pi} \mathbf{B} \cdot \nabla \varphi \, d^3x \\ &= \int_I \frac{1}{8\pi} \mathbf{B} \cdot \mathbf{B} \, d^3x - \int_{\partial(I-II)} \frac{1}{8\pi} \varphi \mathbf{B} \cdot d\mathbf{S}, \end{aligned} \quad (C1)$$

where  $\nabla \cdot \mathbf{B} = 0$  was used. Note that because the  $\hat{\mathbf{n}} \cdot \mathbf{B}$  is continuous across the boundary, this may be evaluated using only type-I quantities.

If  $\Lambda_L$  is defined by  $\mathbf{A} = \mathbf{A}_L + \nabla \Lambda_L$  where  $\mathbf{A}_L$  is in the Lorentz gauge (i.e.,  $\nabla \cdot \mathbf{A}_L = 0$ ), the magnetic helicity is given by

$$\begin{aligned} H &= \int_I \frac{1}{8\pi} \mathbf{A} \cdot \mathbf{B} \, d^3x + \int_{II} \frac{1}{8\pi} \mathbf{A} \cdot \nabla \varphi \, d^3x \\ &= \alpha^{-1} \int_I \frac{1}{8\pi} \mathbf{B} \cdot \mathbf{B} \, d^3x - \int_{\partial(I-II)} \frac{1}{8\pi} \varphi \mathbf{A} \cdot d\mathbf{S} \\ &\quad - \int_{II} \frac{1}{8\pi} \varphi \nabla \cdot \mathbf{A} \, d^3x \\ &= \alpha^{-1} \int_I \frac{1}{8\pi} \mathbf{B} \cdot \mathbf{B} \, d^3x - \alpha^{-1} \int_{\partial(I-II)} \frac{1}{8\pi} \varphi \mathbf{B} \cdot d\mathbf{S} \\ &\quad - \int_{II} \frac{1}{8\pi} \varphi \nabla^2 \Lambda_L \, d^3x \\ &= \alpha^{-1} U + \int_{\partial(I-II)} \frac{1}{8\pi} \varphi \nabla \Lambda_L \cdot d\mathbf{S} + \int_{II} \frac{1}{8\pi} \mathbf{B} \cdot \nabla \Lambda_L \\ &= \alpha^{-1} U - \int_{\partial(I-II)} \frac{1}{8\pi} (\Lambda_L \nabla \varphi - \varphi \nabla \Lambda_L) \cdot d\mathbf{S}, \end{aligned} \quad (C2)$$

where  $\nabla \cdot \mathbf{B} = \nabla \cdot \mathbf{A}_L = 0$  and the continuity of  $\mathbf{A}$  and  $\mathbf{B} \cdot \hat{\mathbf{n}}$  at the boundary were used (i.e., on the boundary  $\hat{\mathbf{n}} \cdot \mathbf{A}_{II} = \hat{\mathbf{n}} \cdot \mathbf{A}_I = \alpha^{-1} \hat{\mathbf{n}} \cdot \mathbf{B}_I = \alpha^{-1} \hat{\mathbf{n}} \cdot \mathbf{B}_{II}$ ). Therefore, the action may be written as

$$S = U - \alpha H = \int_{\partial(I-II)} \frac{\alpha}{8\pi} (\Lambda_L \nabla \varphi - \varphi \nabla \Lambda_L) \cdot d\mathbf{S}, \quad (C3)$$

where  $\varphi$  and  $\Lambda_L$  are implicit functions of  $\alpha$  through equation (5). Note that when  $\Lambda_L$  vanishes, i.e., the force-free gauge is a Lorentz gauge everywhere,  $U = \alpha H$  as found for the Woltjer state.

### APPENDIX D: VECTOR SPHERICAL HARMONICS

Vector spherical harmonics are used extensively, and thus some of their properties are summarized below (see, e.g., Barrera et al. 1985, for more detail). While it is possible to expand the angular dependence of a vector in many ways, simplifications of the Helmholtz equation can be obtained with the following choices:

$$\mathbf{Y}_{lm} \equiv \hat{\mathbf{e}}_r Y_{lm}, \quad \mathbf{\Psi}_{lm} \equiv r \nabla Y_{lm}, \quad \mathbf{\Phi}_{lm} \equiv \mathbf{r} \times \nabla Y_{lm}, \quad (D1)$$

where the  $Y_{lm}$  are the standard scalar spherical harmonics (see Table D1 for explicit expressions for low  $l$ ). These have

the following useful properties:

$$\begin{aligned} \nabla \cdot (F(r) \mathbf{\Phi}_{lm}) &= 0, \\ \nabla \times (F(r) \mathbf{Y}_{lm}) &= -\frac{F(r)}{r} \mathbf{\Phi}_{lm}, \\ \nabla \times (F(r) \mathbf{\Psi}_{lm}) &= \left( \frac{1}{r} \partial_r r F(r) \right) \mathbf{\Phi}_{lm} \\ \nabla \times (F(r) \mathbf{\Phi}_{lm}) &= -\left( \frac{l(l+1)}{r} F(r) \right) \mathbf{Y}_{lm} \\ &\quad - \left( \frac{1}{r} \partial_r r F(r) \right) \mathbf{\Psi}_{lm}. \end{aligned} \quad (D2)$$

They are also orthogonal on the unit sphere:

$$\begin{aligned} \int d\Omega \mathbf{Y}_{lm} \cdot \mathbf{Y}_{l'm'}^* &= \delta_{ll'} \delta_{mm'}, \\ \int d\Omega \mathbf{\Psi}_{lm} \cdot \mathbf{\Psi}_{l'm'}^* &= l(l+1) \delta_{ll'} \delta_{mm'}, \\ \int d\Omega \mathbf{\Phi}_{lm} \cdot \mathbf{\Phi}_{l'm'}^* &= l(l+1) \delta_{ll'} \delta_{mm'}, \\ \int d\Omega \mathbf{Y}_{lm} \cdot \mathbf{\Psi}_{l'm'}^* &= \int d\Omega \mathbf{Y}_{lm} \cdot \mathbf{\Phi}_{l'm'}^* \\ &= \int d\Omega \mathbf{\Psi}_{lm} \cdot \mathbf{\Phi}_{l'm'}^* = 0. \end{aligned} \quad (D3)$$

Note that equation (D2) implies that

$$\nabla \times \nabla \times (F(r) \mathbf{\Phi}_{lm}) = (-\Delta_l F(r)) \mathbf{\Phi}_{lm}, \quad (D4)$$

where  $\Delta_l$  is the 3-dimensional Laplacian associated with the meridional harmonic  $l$ , i.e.,

$$\Delta_l = \frac{1}{r^2} \partial_r r^2 \partial_r - \frac{l(l+1)}{r^2}. \quad (D5)$$

Note that the general solution to  $\Delta_l f + \alpha^2 f = 0$  are the spherical Bessel functions of order  $l$ ,  $j_l(\alpha r)$  and  $n_l(\alpha r)$ . The first few of these are summarized in Table D2, and more information may be found in Abramowitz & Stegun (1972).

### REFERENCES

- Abramowitz M., Stegun I. A., 1972, Handbook of Mathematical Functions. Handbook of Mathematical Functions, New York: Dover, 1972
- Barrera R. G., Estevez G. A., Giraldo J., 1985, European Journal of Physics, 6, 287
- Braithwaite J., Spruit H. C., 2004, Nature, 431, 819
- Braithwaite J., Spruit H. C., 2006, A&A, 450, 1097
- Heidbrink W. W., Dang T. H., 2000, Plasma Physics and Controlled Fusion, 42, L31
- Hsu S. C., Bellan P. M., 2002, MNRAS, 334, 257
- Ji H., Prager S. C., Sarff J. S., 1995, Phys. Rev. Lett., 74, 2945
- Landstreet J. D., Mathys G., 2000, A&A, 359, 213
- Lyutikov M., 2006, MNRAS, 367, 1594
- Spruit H. C., 2002, A&A, 381, 923
- Taylor J. B., 1974, Physical Review Letters, 33, 1139
- Thompson C., Duncan R. C., 1993, ApJ, 408, 194
- Thompson C., Lyutikov M., Kulkarni S. R., 2002, ApJ, 574, 332
- Tout C. A., Wickramasinghe D. T., Ferrario L., 2004, MNRAS, 355, L13

**Table D1.** Explicit expressions for the azimuthally symmetric  $l = 0, 1, 2$  and  $3$  vector spherical harmonics.

$l$	$m$	$\mathbf{Y}_{lm}$	$\mathbf{\Psi}_{lm}$	$\mathbf{\Phi}_{lm}$
0	0	$\sqrt{\frac{1}{4\pi}} \hat{\mathbf{e}}_r$	0	0
1	0	$\sqrt{\frac{3}{4\pi}} \cos \theta \hat{\mathbf{e}}_r$	$-\sqrt{\frac{3}{4\pi}} \sin \theta \hat{\mathbf{e}}_\theta$	$-\sqrt{\frac{3}{4\pi}} \sin \theta \hat{\mathbf{e}}_\phi$
2	0	$\sqrt{\frac{5}{16\pi}} (3 \cos^2 \theta - 1) \hat{\mathbf{e}}_r$	$-\sqrt{\frac{45}{4\pi}} \cos \theta \sin \theta \hat{\mathbf{e}}_\theta$	$-\sqrt{\frac{45}{4\pi}} \cos \theta \sin \theta \hat{\mathbf{e}}_\phi$
3	0	$\sqrt{\frac{7}{16\pi}} (5 \cos^3 \theta - 3 \cos \theta) \hat{\mathbf{e}}_r$	$-\sqrt{\frac{63}{16\pi}} (5 \cos^2 \theta \sin \theta - \sin \theta) \hat{\mathbf{e}}_\theta$	$-\sqrt{\frac{63}{16\pi}} (5 \cos^2 \theta \sin \theta - \sin \theta) \hat{\mathbf{e}}_\phi$

**Table D2.** Explicit expressions for the spherical Bessel functions of orders  $l = 0, 1, 2$  and  $3$  (Abramowitz & Stegun 1972).

$l$	$j_l(z)$	$n_l(z)$
0	$\frac{1}{z} \sin z$	$-\frac{1}{z} \cos z$
1	$\frac{1}{z^2} \sin z - \frac{1}{z} \cos z$	$-\frac{1}{z^2} \cos z - \frac{1}{z} \sin z$
2	$\left(\frac{3}{z^3} - \frac{1}{z}\right) \sin z - \frac{3}{z^2} \cos z$	$-\left(\frac{3}{z^3} - \frac{1}{z}\right) \cos z - \frac{3}{z^2} \sin z$
3	$\left(\frac{15}{z^4} - \frac{3}{z^2}\right) \sin z - \left(\frac{15}{z^3} - \frac{1}{z}\right) \cos z$	$-\left(\frac{15}{z^4} - \frac{3}{z^2}\right) \cos z - \left(\frac{15}{z^3} - \frac{1}{z}\right) \sin z$

Wickramasinghe D. T., Ferrario L., 2005, in Koester D., Moehler S., eds, ASP Conf. Ser. 334: 14th European Workshop on White Dwarfs Fossil Fields in Magnetic White Dwarfs. pp 153–+

Woltjer L., 1958, Proceedings of the National Academy of Science, 44, 489

Woltjer L., 1962, ApJ, 135, 235

Yoshida S., Yoshida S., Eriguchi Y., 2006, ApJ, 651, 462